

This is the accepted manuscript made available via CHORUS. The article has been published as:

Heralded Single Photons Based on Spectral Multiplexing and Feed-Forward Control

M. Grimaud Puigibert, G. H. Aguilar, Q. Zhou, F. Marsili, M. D. Shaw, V. B. Verma, S. W. Nam, D. Oblak, and W. Tittel

Phys. Rev. Lett. **119**, 083601 — Published 25 August 2017

DOI: [10.1103/PhysRevLett.119.083601](https://doi.org/10.1103/PhysRevLett.119.083601)

Heralded single photons based on spectral multiplexing and feed-forward control

M. Grimaud Puigibert,¹ G. H. Aguilar,¹ Q. Zhou,¹ F. Marsili,² M. D. Shaw,² V. B. Verma,³ S. W. Nam,³ D. Oblak,¹ and W. Tittel¹

¹*Institute for Quantum Science and Technology, and Department of Physics & Astronomy, University of Calgary, 2500 University Drive NW, Calgary, Alberta T2N 1N4, Canada*

²*Jet Propulsion Laboratory, California Institute of Technology, 4800 Oak Grove Drive, Pasadena, California 91109, USA*

³*National Institute of Standards and Technology, Boulder, Colorado 80305, USA*

(Dated: July 20, 2017)

We propose and experimentally demonstrate a novel approach to a heralded single photon source based on spectral multiplexing (SMUX) and feed-forward-based spectral manipulation of photons created by means of spontaneous parametric down-conversion in a periodically-poled LiNbO₃ crystal. As a proof-of-principle, we show that our 3-mode SMUX increases the heralded single-photon rate compared to that of the individual modes without compromising the quality of the emitted single-photons. We project that by adding further modes, our approach can lead to a deterministic SPS.

Photonic quantum information processing promises delivering optimal security for sensitive communication [1], solving certain computational problems much faster than classical computers [2, 3], and estimating physical parameters with significantly improved resolution [4]. Many of these applications rely on sources of deterministic (on-demand) and near-perfect single photons [5].

The most common realization of a single-photon source (SPS) is based on the generation of correlated pairs of photons (usually coined idler and signal photons) followed by the detection of one member of the pair (henceforth assumed to be the idler), which heralds the presence of the other. In this scheme, a crucial step is the pair generation process, which is achieved through spontaneous parametric down-conversion (SPDC) or spontaneous four-wave-mixing in a nonlinear optical medium. The experimental simplicity and versatility of such heralded sources have earned them a key role in numerous quantum information applications [6]. In terms of quality, these sources can produce highly indistinguishable photons, but their main limitation lies in the spontaneous nature of the pair generation. Pairs of single photons are generated only with a certain probability $p_{n=1} < 1$ and, moreover, there is a chance of generating multiple photon pairs, which results in multi-photon emission from the SPS (for $p_{n=1} \ll 1$ the probability for generating multiple pairs is $p_{n \geq 2} \approx p_{n=1}^2$) and hence non-pure single photon states. If the collection and detection efficiency of the idler photon is large photon-number resolving detectors [7, 8] will increase the purity, but the maximum single-photon emission probability will still be limited to $p_{n=1} = 0.25$ [9].

An alternative approach to implement SPSs uses single emitters [10] such as diamond colour centers [11], single molecules [12] and quantum dots [13, 14]. Such conceptually simple sources are in principle capable of deterministically emitting a pure single photon within the emitter's excitation lifetime. For diamond colour centers a number of recent experiments has shown nearly pure and indistinguishable photons emitted from separate sources

[15, 16]. If these properties can be combined with the large collection efficiencies demonstrated in other experiments, and emission into phonon side-bands can be suppressed, colour centers have potential to realize ideal SPSs. Furthermore, the rapid progress in fabrication methods and active control of the properties of quantum dots has also yielded photon emitters with high purity, close-to deterministic emission and good indistinguishability, however, only for photons emitted by the same source at different times [17, 42]. Indistinguishability between photons emitted from two independent quantum dots has also been demonstrated, but with low collection efficiency [18]. Yet another shared impediment of all single-emitter sources is the complexity of their fabrication and emission wavelength tuning, and the need for a cryogenic environment.

A promising avenue to overcome the limitations of the above types of sources is based on revisiting the heralded SPSs. The scheme proposed in [19, 20] realizes in principle a deterministic SPS by actively multiplexing many non-deterministic heralded photon sources that emit photons in different modes. In that way one retains the advantageous properties of the HSPS — such as indistinguishability and ability to widely tune the output spectral width and wavelength — while overcoming the limitations to the single photon purity. In the multiplexing scheme, the detection of an idler photon in any mode out of the chosen set heralds the presence of a signal photon in a corresponding optical mode. Then, using a feed-forward signal from the idler photon detector, the signal mode is mapped onto a (predetermined) single mode. In doing so, the probability to generate a single pair in at least one of the modes increases linearly with the number of modes m (for small $p_{n=1}$), and the photon emission probability after feed-forward-based mode mapping of the signal mode can hence be made to approach unity. At the same time, the probability for multi-pair emissions into the feed-forward-mapped output mode also increases proportionally to m , which means that the ratio $p_{n=1}/p_{n=2}$ after mode-mapping, and hence the single-

photon purity, remains constant. Though, initially, this seems unsatisfactory, it turns out to be far superior to the scaling for an individual heralded SPS. In this case, if the same increase of $p_{n=1}$ by a factor of $k = m$ were to be achieved by increasing the SPDC pump-power, it would result in an increase of $p_{n \geq 2}$ by a factor of k^2 . Hence the ratio $p_{n=1}/p_{n=2} \propto 1/k$. In other words the non-multiplexed HSPS would produce more and more multi-photons as the emission rate is increased.

Multiplexed heralded sources have thus far been realized using spatial [21–23], temporal [24] and spatio-temporal modes [25]. In some cases, they have shown to outperform non-multiplexed sources in terms of throughput and quality. However, scaling up the number of modes in the employed degrees of freedom requires more resources, and generally impacts the overall performance. In the case of spatial multiplexing, each additional mode requires an independent source and an added switching connection that induces some amount of extra loss [26]. Temporal multiplexing does not necessarily consume more physical resources but does inevitably encroach on the repetition rate of the source and hence limits the single photon throughput.

Here, we propose and demonstrate an SPS based on a novel spectral multiplexing (SMUX) scheme in which the source requirements and the system loss are independent of the number of modes being multiplexed. The scheme is based on defining spectral modes within the broadband spectrum of an SPDC pair source and applying a feed-forward frequency-shift operation on the heralded photon. We experimentally show that the single-photon character is preserved by measuring a heralded autocorrelation function $g_{H,0}^{(2)} \ll 1$ for the heralded photons with and without multiplexing and feed-forward control. Moreover, directly comparing the multiplexed and non-multiplexed output we deduce that, as expected, the heralded single-photon emissions increase linearly with the number of modes. This allows compensating for the additional loss caused by the non-ideal elements used for the feed-forward operation for as few as three modes.

The experimental implementation of the scheme is shown in Fig. 1a. A pulsed laser (80 MHz repetition rate) creating 18 ps-long pulses centred at 523.5 nm wavelength, with average power of 7 mW, pumps a 2 cm long periodically-poled lithium-niobate (PPLN) crystal to produce 350 GHz-wide, frequency non-degenerate photon pairs, each composed of a signal photon centred at 795 nm and an idler at 1532 nm. The spectral distribution of the pairs is conveniently illustrated by their joint spectral amplitude (JSA) shown in Fig. 1b. The JSA represents the probability amplitude to detect a pair of photons centered at the frequencies ν_s and ν_i . Since each pair of photons has to satisfy energy conservation, the JSA is confined to the diagonal band (green region), whose cross-sectional width is given by the spectral width of the pump laser $\delta\nu_p$. (Under our experimental conditions the phase-matching condition is less restrictive than the energy conservation and thus phase-matching is not

considered in the pictorial representation)

Both signal and idler modes are coupled into single mode fibers (the number of detected photon pairs before any spectral filtering is 640 kHz). Subsequently, the signal photons are transmitted to an optical delay line while the idler photons exit the optical fiber and are sent to a pair of orthogonally oriented 50×50 mm square diffraction gratings (DGs, 600 lines/mm) that map photons with spectra centred at $\nu_{i0} = 195.612$ THz (1532.59 nm), $\nu_{i+} = \nu_{i0} + 19$ GHz (1532.44 nm) and $\nu_{i-} = \nu_{i0} - 22$ GHz (1532.76 nm), each featuring a spectral width of 12 GHz [27], onto distinct spatial modes. In the JSA of Fig. 1b these idler spectral modes are highlighted as orange (middle), yellow (upper) and red (lower) horizontal bands. The idler photons in each mode are detected using WSi superconducting nanowire single-photon detectors (SNSPDs) cooled to 700 mK in a closed-cycle cryostat. When an idler photon is detected in mode ν_{i+} , ν_{i0} or ν_{i-} , it heralds the presence of a signal photon with a central frequency of $\nu_{s0} = 377.059$ THz (795.08 nm), $\nu_{s+} = \nu_{s0} - 19$ GHz (795.12 nm) or $\nu_{s-} = \nu_{s0} + 22$ GHz (795.03 nm), respectively.

The heralding signals from the output of the SNSPDs are processed by a logic circuit that triggers the creation of a feed-forward signal in the form of a 700 ps long pulse with suitable, linearly changing voltage. This ramp signal is applied to the electrical input of a lithium-niobate (LiNbO_3) phase-modulator (LN-PM) that is optically connected to the output of the 512 ns-duration delay line for the signal-photon. As is shown in [27] the resulting linear phase-ramp applied during the passage of the signal photon actively shifts the spectrum of the heralded signal photon to a spectral band — shown as vertical blue area in the JSA — determined by the transmission of a Fabry Perot cavity (FP) with bandwidth $\delta\nu_s = 6$ GHz. Note that the frequency shifts are applied to the entire spectrum of the signal photons, as indicated by the dotted arrows in Fig. 1b. As a consequence, signal photons not corresponding to the heralded spectral band are shifted out of the cavity resonance and thus rejected. Finally, the signal photons are detected by a silicon avalanche photodiode (APD) and another logic circuit records coincidences with the heralding signals from all SNSPDs.

We first characterize the spectral difference between signal photons depending on which idler photon serves as a herald. Towards this end we measure the heralded single photon rates for each idler frequency mode (ν_{i+} , ν_{i0} and ν_{i-}) while tuning the resonance frequency of the FP cavity that acts on the signal photon. To centre the spectral transmission of the FP at ν_{s0} , we maximize the coincidence counts when heralding exclusively with idler photons detected in mode ν_{i0} . Note that although the LN-PM is part of the measurement set-up, it is not active. The results are shown in Fig. 2a. For all modes, we measure bandwidths of the heralded photon spectra of around 37 GHz, which matches the convolution of the pump laser bandwidth $\delta\nu_p = 24$ GHz with the filter

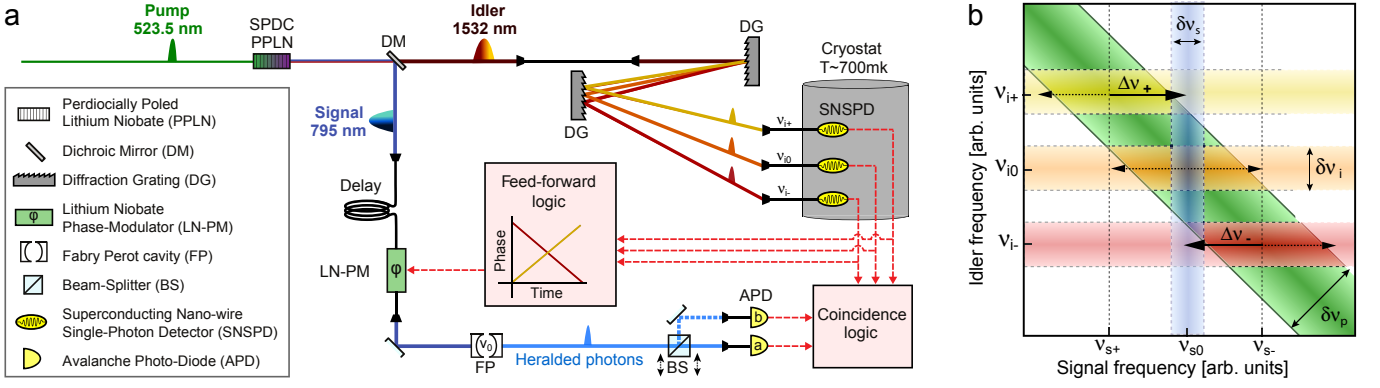


FIG. 1: **a. Schematic of experimental setup.** **b. Illustration of concept using the Joint spectral amplitude** Details in the main-text

bandwidths $\delta\nu_s = 6$ GHz and $\delta\nu_i = 12$ GHz. Furthermore, we find that the maximum coincidence rate for each pair of photons is at the relative frequency differences of $\Delta\nu_- = -19$ GHz and $\Delta\nu_+ = +22$ GHz.

Next, we assess the performance of the linear ramp frequency shifting (LRFS) by again recording the heralded-photon spectra for each idler frequency-mode, but now with the corresponding feed-forward signal applied to the LN-PM. For these measurements, the resonance frequency of the FP cavity remains fixed at ν_{s0} . As expected, the spectra shown in Fig. 2b now completely overlap. Moreover, by comparing with the results in Fig. 2a, we observe that the detection rates with and without LRFS are essentially equal. This shows that our setup is capable of applying the on-demand frequency shift at the single-photon level with nearly 100% efficiency.

Now we activate the full setup and evaluate the performance of our frequency multiplexed heralded source in view of the requirements of an ideal single photon source. First, we measure the heralded single photon (HSP) rate as a function of the pump power with and without multiplexing. The red, yellow and orange circles in Fig. 3 show the rates of signal photons (after spectral filtering by the FP cavity) heralded by the individual frequency modes at ν_{i+} , ν_{i0} and ν_{i-} . The multiplexed HSP rate for the SMUX source (green circles) is about 2.7 times larger than that of the average of the individual sources, i.e. a significant improvement over that for the individual modes. Yet, to make a fair comparison of the effect of the SMUX, we compare the multiplexed HSP rate to the rate when heralding with only the ν_{i0} mode and with the LN-PM removed, which, for the specific modulator used in our experiment, adds 5 dB loss and is not needed in the case of using only a standard HSPS without multiplexing. However, we keep the spectral filtering elements on both idler and signal fields as these are necessary to achieve pure states [36]. The rate obtained with the thus modified source (purple circles) is similar to the SMUX rate, which can be explained by the increased transmission due to having removed the LN-PM compensating for the lack of multiplexing. Hence, in our experiment,

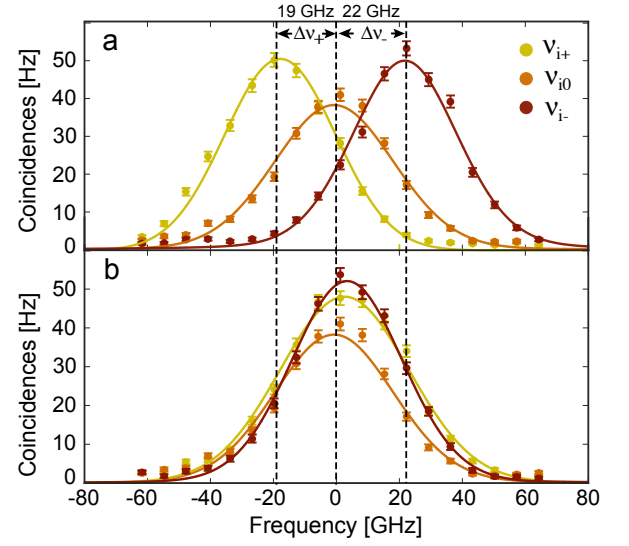


FIG. 2: Coincidences count rates without (a) and with (b) frequency shifting. The horizontal axis correspond to the relative frequency difference of the cavity resonance with respect to ν_{s0} . Coincidence rates between the signal and (heralding) idler photons at frequencies ν_{i+} , ν_{i0} and ν_{i-} are presented in yellow, orange and red, respectively. The solid lines are fits using $\mathcal{F} = \mathcal{G}_{\nu_s} \star \mathcal{H}_{\nu_i} \star \mathcal{I}_{\nu_p}$, where \mathcal{G}_{ν_s} is a Lorentzian function describing the frequency response of the FP cavity; \mathcal{H}_{ν_i} and \mathcal{I}_{ν_p} are Gaussians characterizing the filtering by the DGs and the spectrum of the pump laser, respectively; and \star denotes convolution.

which employs 3 modes, spectral multiplexing does not yet create an advantage in view of the HSP rate and in creating a deterministic source. However, we emphasize that increasing the number of modes would neither increase the system loss nor require additional elements in the signal mode. Hence, we can assume that the HSP rate will continue to increase as more spectral modes are added, rapidly surpassing that of the non-multiplexed source.

Next, we verify that multiplexing maintains the single photon character of our light source. One of the most

common methods for this is to determine its purity [42], which, for a heralded source, is generally quantified in terms of its heralded auto-correlation function. To measure this, we direct the heralded signal photons after the FP cavity through a 50/50 beam splitter (BS), and record the individual counts $C_H^{(i)} (i \in \{a, b\})$ in, as well as coincidences $C_H^{(ab)}$ between, the APDs — labelled a and b — placed at its two outputs (see Fig. 1a). Denoting the total number of heralding signals, H , we define the heralded auto-correlation as $g_H^{(2)}(0) = C_H^{(ab)} H / (C_H^{(a)} C_H^{(b)})$ [27]. Since detection in both detectors can only occur if two or more photons are present, we expect $C_H^{(ab)} / H \approx p_{n=2}^H / 2$, where $p_{n=2}^H$ is the heralded two-photon probability. On the other hand, the individual detector counts are dominated by single photon events such that e.g. $C_H^{(a)} / H \approx p_{n=1}^H / 2$ (assuming $p_{n=1}^H \gg p_{n=2}^H$). Clearly these considerations hold for the multiplexed and non-multiplexed sources alike [27]. Hence, the autocorrelation function is approximated by $g_H^{(2)}(0) \approx 2p_{n=2}^H / (p_{n=1}^H)^2$, which provides a direct relation to the photon-statistics. In particular, $g_H^{(2)}(0) \sim 0$ would indicate $p_{n=2}^H \sim 0$ and $p_{n=1}^H > 0$.

Operating the source at maximum power with the LN-PM (and hence the multiplexing) removed, we obtain a value of $g_H^{(2)}(0) = 0.05 \pm 0.01$. With the SMUX activated and using the same pump power, we measure $g_H^{(2)}(0) = 0.06 \pm 0.01$, which equals the value without multiplexing within experimental uncertainty. If the LN-PM loss were lower we would thus achieve a larger HSP rate without increasing the $g_H^{(2)}(0)$ [27]. Both experimentally measured $g_H^{(2)}(0) \ll 1$, which indicates a highly pure single photon character of the output mode. Hence, we establish that the SMUX maintains the single photon nature of the source. This conclusion is supported by additional measurements of the so-called coincidence to accidental ratio (CAR) measured with and without the SMUX [28].

We did not directly measure the degree of distinguishability of single photons from our source, but based on the experimental setup, we conjecture they must be nearly indistinguishable. The reason for this is that the photons emitted by our SMUX source pass through a FP-cavity and are coupled into single mode fibre, which removes any distinguishability in the frequency and spatial degrees of freedom. Finally, the fact that all signal photons travel along the same path, from the point where they are created to the point where they are detected, means that their arrival times and polarization are the same (irrespective of which spectral mode they belong to), provided that chromatic dispersion and polarization mode dispersion can be ignored.

In conclusion, we have introduced the idea of a spectrally multiplexed SPS and experimentally demonstrated that multiplexing three spectral modes leads to the expected increase in the heralded single photon rate while keeping the purity constant. To achieve these results we

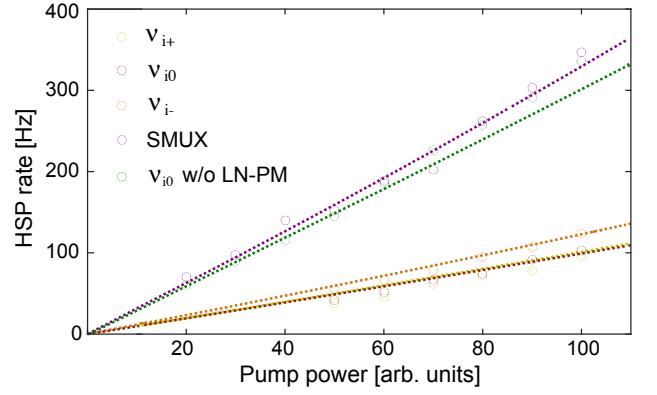


FIG. 3: **a** HSP rate versus pump power for the individual frequency modes (red, yellow and orange circles), for SMUX of three modes (green circles) and for the ν_0 mode without the LN-PM in the signal photon mode (purple circles). Lines are linear fits to the data.

have implemented on-demand frequency shifting of single photons over approximately ± 20 GHz with nearly 100% efficiency by driving a commercially available LiNbO₃ phase modulator with a linear voltage ramp. This technical advance also finds application in the proposed spectrally multiplexed quantum repeater protocols [40].

There is a number of avenues to increase the heralded single-photon rate of our source. An evident path is to reduce the loss incurred by imperfect components, spectral mismatch between the filters and the SPDC pump, and imperfect coupling of the SPDC output modes. For instance, employing phase-modulator with a realistic lower loss of 1.5 dB would yield a 2.5 times improvement of the HSP rate.

Also, cavity-enhanced SPDC would allow one to define the spectral modes for the multiplexing, and thus remove loss due to spectral narrowing [29]. In addition, the increased efficiency of the SPDC process in the cavity would demand less pump power [27]. Finally, the spatial mode matching of the SPDC output to optical fibers would also be assisted by cavity enhanced SPDC, in particular if integrated with a waveguide-patterned nonlinear crystal [30, 31].

At a more fundamental level, more spectral modes must be multiplexed. This can be achieved both by increasing the spectral mode density (e.g. using commercially available ultra-dense wavelength division multiplexers with 6 GHz bandwidth), as well as by improving the total bandwidth — the latter necessitating improvement of the maximum frequency shifts by using higher-bandwidth electronics [32, 33, 38, 39]. Assuming 6 GHz wide spectral channels and an 8-fold increase of the shifting range to 350 GHz (the spectral width of the photon-pairs created by our source), it is feasible to reach 60 spectral channels. This will suffice for creating at least one heralding event per pump pulse and for making the source as close to deterministic as allowed by the loss in the signal path [9], which is independent of the num-

ber of multiplexed modes. Changing the length of the non-linear crystal and phase-matching conditions an even broader SPDC spectrum and thus more modes may be feasible.

Acknowledgments

The authors thank Vladimir Kiselyov for technical support and Raju Valivarthi for discussions. This work was funded through Alberta Innovates Technology Futures

(AITF), and the National Science and Engineering Research Council of Canada (NSERC). VBV and SWN acknowledge partial funding for detector development from the Defense Advanced Research Projects Agency (DARPA) Information in a Photon (InPho) program. Part of the detector research was carried out at the Jet Propulsion Laboratory, California Institute of Technology, under a contract with the National Aeronautics and Space Administration. WT furthermore acknowledges funding as a Senior Fellow of the Canadian Institute for Advanced Research (CIFAR).

-
- [1] N. Gisin and R. Thew, *Nat. Phot.* **1**, 165-171 (2007).
 - [2] P. W. Shor, *SIAM J. Comput.* **26**, 1484 (1997).
 - [3] T. D. Ladd, F. Jelezko, R. Laflamme, Y. Nakamura, and C. Monroe, *Nature* **464**, 4553 (2010).
 - [4] V. Giovannetti, S. Lloyd, and L. Maccone, *Phys. Rev. Lett.* **96**, 010401 (2006).
 - [5] E. Knill, R. Laflamme, and G. Milburn, *Nature* **409**, 46-52 (2001).
 - [6] J. W. Pan, Z. B. Chen, C. Y. Lu, H. Weinfurter, A. Zeilinger, and M. Zukowski, *Rev. Mod. Phys.* **84**, 777-838 (2012).
 - [7] A. E. Lita, A. J. Miller, and S. W. Nam, *Optics Express* **16**, 5, 3032-3040 (2008).
 - [8] M. S. Allman, V. B. Verma, M. Stevens, T. Gerrits, R. D. Horansky, A. E. Lita, F. Marsili, A. Beyer, M. D. Shaw, D. Kumor, R. Mirin and S. W. Nam, *Appl. Phys. Lett.* **106**, 192601 (2015).
 - [9] A. Christ and C. Silberhorn, *Phys. Rev. A* **85**, 023829 (2012).
 - [10] I. Aharonovich, D. Englund, and M. Toth, *Nat. Phot.* **10**, 631-641 (2016).
 - [11] T. M. Babinec, B. J. M. Hausmann, M. Khan, Y. Zhang, J. R. Maze, P. R. Hemmer, and M. Loncar, *Nat. Nano.* **5**, 195-199 (2010).
 - [12] B. Lounis and W. E. Moerner, *Nature* **407**, 491-493 (2000).
 - [13] P. Michler, A. Kiraz, C. Becher, W. V. Schoenfeld, P. M. Petroff, Lidong Zhang, E. Hu, and A. Imamoglu, *Science* **290**, 2282-2285 (2000).
 - [14] A. J. Shields, *Nat. Phot.* **1**, 215-223 (2007).
 - [15] W. Pfaff, B. J. Hensen, H. Bernien, S. B. van Dam, M. S. Blok, T. H. Taminiau, M. J. Tiggelman, R. N. Schouten, M. Markham, D. J. Twitchen, R. Hanson, *Science* **345**:6196, 532-535 (2014)
 - [16] A. Sipahigil, K.D. Jahnke, L.J. Rogers, T. Teraji, J. Isoya, A.S. Zibrov, F. Jelezko, and M.D. Lukin, *Phys. Rev. Lett.* **113**, 113602 (2014).
 - [17] X. Ding, Y. He and Z.-C. Duan and N. Gregersen and M.-C. Chen, S. Unsleber, S. Maier, C. Schneider, M. Kamp, S. Höfling and C.-Y. Lu and J.-W. Pan, *Phys. Rev. Lett.*, **116**, 020401 (2016).
 - [18] W.B. Gao, P. Fallahi, E. Togan, A. Delteil, Y.S. Chin, J. Miguel-Sanchez and A. Imamoglu, *Nat. Comm.* **4** 2744 (2013).
 - [19] A. L. Migdall, D. Branning, and S. Castelletto, *Phys. Rev. A* **66**, 053805 (2002).
 - [20] J. H. Shapiro and F. N. Wong, *Opt. Lett.* **32**, 2698-2700 (2007).
 - [21] X.-S. Ma, S. Zotter, J. Kofler, T. Jennewein, and A. Zeilinger, *Phys. Rev. A* **83**, 043814 (2011).
 - [22] M. J. Collins, C. Xiong, I. H. Rey, T. D. Vo, J. He, S. Shahnia, C. Reardon, M. J. Steel, T. F. Krauss, A. S. Clark, and B. J. Eggleton, *Nat. Comm.* **4**, 2582 (2013).
 - [23] R. J. A. Francis-Jones, R. A. Hoggarth, and P. J. Mosley, *Optica* **3**, Issue 11, 1270-1273 (2016).
 - [24] C. Xiong, X. Zhang, Z. Liu, M. J. Collins, A. Mahendra, L. G. Helt, M. J. Steel, D.-Y. Choi, C. J. Chae, P. H. W. Leong, and B. J. Eggleton, *Nat. Comm.* **7**, 10853 (2016).
 - [25] G. J. Mendoza, R. Santagati, J. Munns, E. Hemsley, M. Piekarek, E. Martín-López, G. D. Marshall, D. Bonneau, M. G. Thompson, and J. L. O'Brien, *Optica* **3**, 127-132 (2016).
 - [26] D. Bonneau, G. J. Mendoza, J. L. O'Brien, and M. G. Thompson, *New J. Phys.* **17**, 043057 (2015).
 - [27] See Supplemental Material, which includes Refs. [34-43].
 - [28] Manuscript in preparation
 - [29] J. Jin, M. Grimau Puigibert, L. Giner, J. A. Slater, M. R. E. Lamont, V. B. Verma, M. D. Shaw, F. Marsili, S. W. Nam, D. Oblak, and W. Tittel *Phys. Rev. A* **92**, 012329 (2015)
 - [30] Z. Vernon, M. Menotti, C. C. Tison, J. A. Steidle, M. L. Fanto, P. M. Thomas, S. F. Preble, A. M. Smith, P. M. Alsing, M. Liscidini, and J. E. Sipe, *arXiv:1703.10626* (2017)
 - [31] M. Bock and A. Lenhard and C. Chunnillall and C. Becher, *Opt. Express*, **24**, 23992-24001, (2016)
 - [32] Q. Li, M. Davano, and K. Srinivasan, *Nat. Phot.* **10**, 406-414 (2016)
 - [33] B. Albrecht, P. Farrera, X. Fernandez-Gonzalvo, M. Cristiani, and H. de Riedmatten, *Nat. Comm.* **5**, 3376 (2014).
 - [34] www.horiba.com/scientific/products/optics-tutorial/diffraction-gratings/, visited november 2016.
 - [35] J. Moreno, S. Rodriguez-Benavides and, A. B. U'Ren, *Laser Phys.* **20**, 1221 (2010).
 - [36] P. J. Mosley, J. S. Lundeen, B. J. Smith and, I. A. Walmsley, *New Journal of Physics*, **10** (2008).
 - [37] B. Brecht, D. V. Reddy, C. Silberhorn, and M. Raymer, *Phys. Rev. X* **5**, 041017 (2015).
 - [38] L. J. Wright, M. Karpinski, C. Söller and B. J. Smith, *arXiv:1605.00640v1*, (2016).
 - [39] L. Fan, C. Zou, M. Poot, R. Cheng, X. Guo, X. Han, and Hong X. Tang, *Nat. Phot.* **10**, 766-770 (2016).
 - [40] N. Sinclair, E. Saglamyurek, H. Mallahzadeh, J. A. Slater, M. George, R. Ricken, M. P. Hedges, D. Oblak, C.

- Simon, W. Sohle, and W. Tittel, Phys. Rev. Lett. **113**, 053603 (2014)
- [41] E. Saglamyurek, M. Grimaud Puigibert, Q. Zhou, L. Giner, F. Marsili, V. B. Verma, S. W. Nam, L. Oesterling, D. Nippa, D. Oblak and, W. Tittel, Nature Communications **7**, 11202 (2016).
- [42] N. Somaschi, V. Giesz, L. De Santis, J. C. Loredano, M. P. Almeida, G. Hornecker, S. L. Portalupi, T. Grange, C. Antn, J. Demory, C. Gmez, I. Sagnes, N. D. Lanzillotti-Kimura, A. Lematre, A. Auffeves, A. G. White, L. Lanco, and P. Senellart, Nat. Phot., **10** 340-345, (2016).
- [43] P. Sekatski, N. Sangouard, F. Bussières, C. Clausen, N. Gisin and H. Zbinden Journal of Physics B, **45** (2012).